



Developing a New Artificial Intelligence Framework to Estimate the Thalweg of Rivers

Zohre Aghamolaei¹ · Masoud-Reza Hessami-Kermani¹

Received: 6 July 2023 / Accepted: 26 September 2023 / Published online: 25 October 2023
© The Author(s), under exclusive licence to Springer Nature B.V. 2023

Abstract

Hydrographic operations to investigate the riverbed form throughout the entire length of a river are costly and time-consuming. This has made scholars use a wide range of alternative methods to address the issue. In the present study, however, a new framework using Artificial Intelligence (AI) based models is introduced to identify the thalweg of rivers, which provides an accurate estimate of a river thalweg via linking coordinates of their left and right banks. In this regard, we trained and tested the performance of two AI-based models, including Artificial Neural Network (ANN) and Adaptive Neuro-Fuzzy Inference System (ANFIS) models. The database of two rivers, namely the Qinhe River in China and the Gaz River in Iran was used to help evaluate the developed model. Outcomes of the two investigated case studies demonstrated that the values of the statistical error estimators, including the Root Mean Square Error (RMSE) of the ANFIS model were less than those of the ANN model. As a result, the ANFIS model can lead to more accurate results than the ANN model, and it is suitable for cases with less available data. Moreover, comparing the results from the developed models with those of the River Channel Morphology Model (RCMM) showed that AI-based models outdo numerical approaches in the identification of the thalweg of rivers. All in all, it is inferred that the proposed approach not only helps us achieve an accurate geometry of rivers but reduces the side costs and can be used as an effective alternative to field operations. The applicability of the proposed models to different river systems is also discussed as a potential direction for future research.

Keywords Thalweg · Hydraulic geometry relationships · Artificial Intelligence · ANFIS · ANN · Gaz River

✉ Masoud-Reza Hessami-Kermani
hessami@uk.ac.ir

Zohre Aghamolaei
Zohre.aghamolaei@eng.uk.ac.ir

¹ Department of Civil Engineering, Faculty of Engineering, Shahid Bahonar University of Kerman, Kerman, Iran

1 Introduction

Rivers are considered among the major water supply sources in many parts of the world. They undergo a variety of changes due to erosion and sedimentation. Studying changes in the geometrical and morphological characteristics of rivers under the influence of hydrodynamic phenomena such as sediment transport, tides, and salinity changes requires an in-depth understanding of these phenomena (Sharifi et al. 2021). Meticulous examination and prediction of the changes will significantly increase the safety of the constructions along rivers. On the other hand, a lack of knowledge about these phenomena can impose heavy damages and costs on projects (Li et and Heap 2011). Therefore, recognition of flows' hydraulic properties through hydrodynamic analysis is vital in designing and operating the hydraulic structures located around and along rivers, especially in times of floods (Hardy et al. 1999; Raber et al. 2007; Podhornyi et al. 2013). Numerical models have several advantages over physical models when it comes to simulating the behavior of coastal systems. Numerical models are easier to implement and modify, as they only require software and hardware resources, while physical models need laboratory facilities and equipment. Numerical models can also handle a wide range of flow parameters and scenarios, such as different wave conditions, water levels, and sediment characteristics, while physical models are limited by scaling issues and experimental constraints. Furthermore, numerical models are more cost-effective and time-efficient than physical models, as they do not involve physical construction, maintenance, and measurement of the model domain. Therefore, numerical models are preferred for studying complex and dynamic coastal processes (Larson 2005; Quarteroni and Quarteroni 2009).

The accuracy of the results of numerical hydrodynamic flow modeling is a function of the correctness of the riverbed's topographic data (Lai et al. 2018). The most common method for investigating the topography of a river's physical model is to use the data collected for bathymetry using the SoNARs (Sound Navigation and Ranging) method (Intelmann 2006; Nitrouer et al. 2008; Colbo et al. 2014). This approach is very accurate and capable of producing topographic data of the riverbed with high quality and clarity. Nevertheless, the SoNARs method is so costly and lacks accuracy in shallow water conditions (Lai et al. 2018). Thus, various studies have been conducted to introduce inexpensive and accurate methods for bathymetry operations during the past few years. Mervade et al. (2005), for example, introduced a model based on establishing relationships between geometric properties, bottom-line position, and cross-sections of rivers. Lai et al. (2018) proposed an efficient model using Laplace's theory and network generation using elliptical theory for flow lines to reconstruct the geometric sections of rivers. The information about a river in China was also used to validate the model. The results revealed that the model could estimate the longitudinal section of the river based on the information on cross-sections. Other methods presented include interpolation methods such as the kriging method (KM), inverse distance weighting technique (IDW), and nearest neighbor model (NN), which are based on historical data and interpolation of other points in the riverbed. Interpolation methods outperformed the traditional ones (Vogel and Mrker 2010; Li and Heap 2011; Bailly du Bois 2012). Since the historical data on a river's geometry are scarce in some cases, and the available data are only related to cross-sections, it is challenging to find new points for river geometry, and therefore, accurate results cannot be expected. This leads to an urgent need in developing methods that can model river bathymetry in different conditions with high accuracy. Yongfei Fu et al. (2022), Using Fuzzy Comprehensive Evaluation Model in Xiaoqing River, Eastern China for assessment of a multifunctional river.

In recent years, methods based on soft computing and artificial intelligence have overcome the weakness of traditional methods in estimating and modeling many complex phenomena (Riahi-Madvar et al. 2021; Mai et al. 2020; Ben Seghier et al. 2021; Rad et al. 2022; Jafari-Asl et al. 2021a; Rahmanshahi et al. 2023). Artificial Neural Networks (ANNs), support vector machine (SVM), response surface method (RSM), gene expression programming (GEP), adaptive network-based inference system (ANFIS), and multivariate adaptive regression spline (MARS) are among these approaches. Among all, ANN and ANFIS are very popular with users thanks to their ease of use, flexibility, and high accuracy. Hence, many attempts have been made to apply ANN and ANFIS in hydraulic engineering. For instance, they have been used for flow estimation in rivers, design of hydraulic structures, modeling evaporation from the surfaces of rivers and lakes, groundwater level estimation, and water quality modeling (Afzali Ahmadabadi et al. 2023; Jafari-Asl et al. 2021b; Seo et al. 2015; Dikshit et al. 2020; Modaresi et al. 2018; Ebtehaj et al. 2020; Babaei et al. 2018; Ohadi and Jafari-Asl 2021; Walton et al. 2019; Langridge et al. 2020).

However, no comprehensive study has yet been conducted using these two methods to solve the problem of bathymetry in rivers. Thus, the present study was undertaken to present a new approach based on AI models, including ANFIS and ANN, for the accurate estimation of river geometry. To the best knowledge of the authors, the capability of ANN and ANFIS models has not been previously investigated for modeling the bathymetry of rivers. The rest of this paper is organized as follows: The theory of ANFIS, ANN, River Channel Morphology Model (RCMM), and details of the case study are proffered in Section 2. The results of the proposed framework are presented and analyzed in Section 3. A comparative study is carried out in Section 4. Finally, in Section 6, conclusions and future work are given.

2 Methodology

2.1 Artificial Neural Network (ANN)

Typically, an ANN consists of three layers, including input, hidden, and output layers. The outputs of the first layer are the inputs of the second layer, and the layers mediating the input and output layers are called the hidden layer. Each hidden layer is made up of a set of neurons responsible for performing calculations (Noori and Kalin 2016). ANN utilizes a supervised learning technique for training. Network training aims to learn the law between the neurons and provide a suitable output for each input after proper training, which requires adequate adjustment of network weights.

In the training process, the predicted values are compared with the actual values in each iteration the network is run in order to achieve the least error. Then, if an error occurs, the weighting coefficients of the input vectors are corrected. The neurons in the hidden layer are added as a bias according to Eq. (1).

$$y_0 = \sum_{i=1}^n W_i X_i + b \quad (1)$$

where W_i is the weight of the connection branch for input X_i and b is the bias of the network.

If we use a nonlinear transfer function (also known as the activation function), the output value is calculated based on Eq. (3).

$$f(X) = \frac{1}{1 + e^{-X}} \quad (2)$$

$$y_0 = f(X) \sum_{i=1}^n W_i X_i + b \quad (3)$$

Finally, the ANN equation is represented by the following mathematical equation:

$$y_0 = f \left[\sum W O_{kj} \sum W I_{ij} X_i + b_1 \right] + b_2 \quad (4)$$

Determining the optimal number of neurons is of particular importance in network training (Ben Seghier et al. 2021). Many of them will cause overfitting, while a small number will result in underfitting. The optimal number is usually a result of sensitivity analysis. It is noteworthy that an activation function (often sigmoid, tangent, or linear) is used in an ANN to create a connection between inputs and outputs. Figure 1 shows the overall structure of an ANN.

2.2 Adaptive Neuro-Fuzzy Inference System (ANFIS)

ANFIS is a neural network based on Mamdani and Sugeno Fuzzy Inference Systems. Mamdani fuzzy inference was first introduced as a method to create a control system by synthesizing a set of linguistic control rules obtained from experienced human operators. In a Mamdani

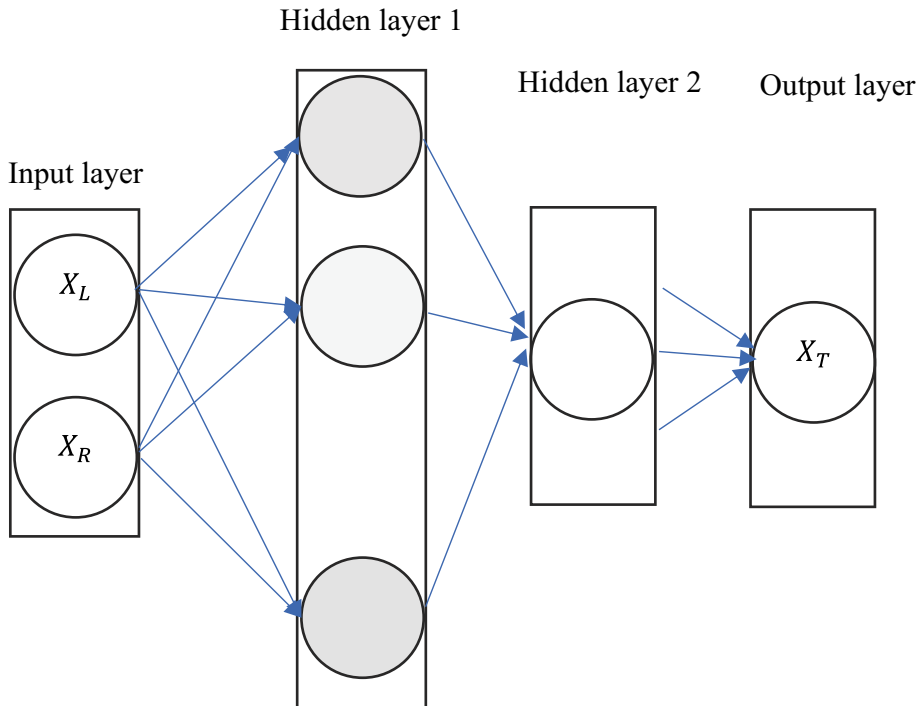


Fig. 1 A schematic structure of ANN

system, the output of each rule is a fuzzy set. Since Mamdani systems have more intuitive and easier to understand rule bases, they are well-suited to expert system applications where the rules are created from human expert knowledge, such as medical diagnostics. The output of each rule is a fuzzy set derived from the output membership function and the implication method of the FIS. These output fuzzy sets are combined into a single fuzzy set using the aggregation method of the FIS. Then, to compute a final crisp output value, the combined output fuzzy set is defuzzified using one of the methods described in Defuzzification Methods. Sugeno fuzzy inference, also referred to as Takagi-Sugeno-Kang fuzzy inference, uses singleton output membership functions that are either constant or a linear function of the input values. The defuzzification process for a Sugeno system is more computationally efficient compared to that of a Mamdani system, since it uses a weighted average or weighted sum of a few data points rather than compute a centroid of a two-dimensional area. In the current research, we use S Sugeno fuzzy inference system, which combines ANN and FIS in a coordinated structure. The ANFIS architecture consists of 5 layers, as shown in Fig. 2. The nodes of the first layers are adaptive, while the other nodes are fixed. If x is equal to A_1 and y is equal to B_1 , the first rule is as follows (Riahi-Madvar et al. 2021):

$$f = p_1x + q_1y + r_1 \quad (5)$$

If x is equal to A_2 and y is equal to B_2 , the second rule is as follows:

$$f = p_2x + q_2y + r_2 \quad (6)$$

where r and q are parameters that must be determined during the ANFIS training process. The application of different layers of ANFIS is presented in Eqs. (7) and (8).

$$Q_{1,i} = \sigma_{A_{i(x)}} \quad (7)$$

$$Q_{1,i} = \sigma_{B_{i(x)}} \quad (8)$$

where A_i is the linguistic variable, x is the input of node i and Q_j , and i is the membership function of A_i , which is usually defined as the Gaussian function (Eq. 9).

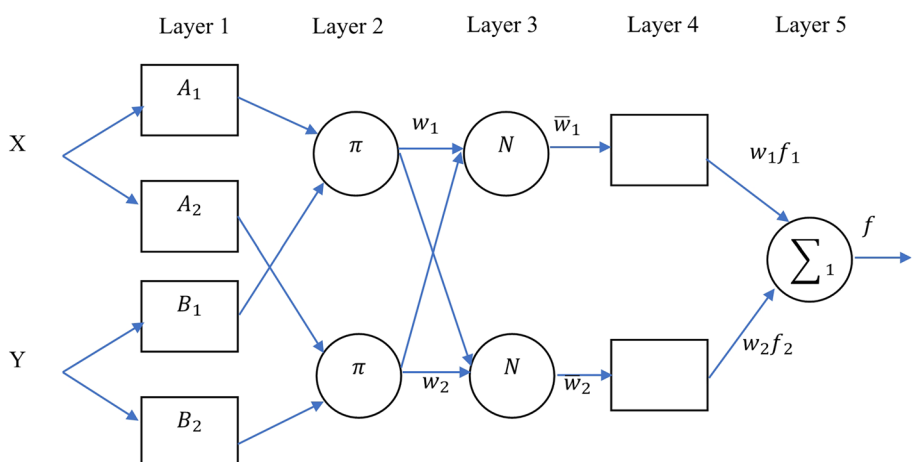


Fig. 2 A schematic structure of ANFIS

$$\sigma_{A_{i(x)}} = \exp\left(\frac{-(x - c)^2}{\sigma^2}\right) \quad (9)$$

where σ is the standard deviation and C is the center of the Gaussian membership function. In the second layer, the excitation intensity of each principle is presented in Eq. (10).

$$w_i = \sigma_{A_{i(x)}} \times \sigma_{B_{i(x)}}, i = 1, 2 \quad (10)$$

In the third layer, the excitation intensity of each rule is calculated as follows:

$$\bar{w} = \frac{w_i}{w_1 + w_2} \quad (11)$$

In the fourth layer, the sum of fuzzy rules is calculated according to Eq. (12):

$$\bar{w}_i f_i = \bar{w}_i (p_i x + q_i y + r_i) \quad (12)$$

In the fifth layer, all outputs of the fourth layer are summed as follows:

$$\sum_i \bar{w}_i f_i = \frac{\bar{w}_i f_i}{\sum_i \bar{w}_i} \quad (13)$$

In the proposed thalweg modeling approach of the present study, as shown in Fig. 3, the geographic coordinates of the right and left banks of a river (X_s , Y_s , and Z_s) are used to estimate the geographic coordinate of the thalweg (X , Y , and Z), respectively.

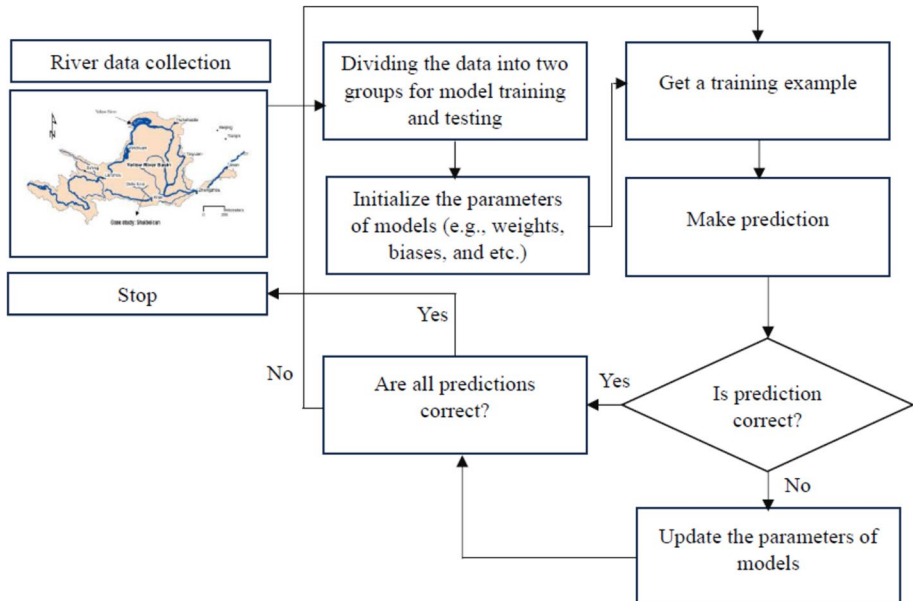


Fig. 3 Flowchart of proposed AI-based model

2.3 River Channel Morphology Model (RCMM)

RCMM is an efficient conceptual model for estimating the thalweg of rivers. This model uses the information of a river's planform to simulate the topography (Merwade et al. 2005). In brief, the erosion and deposition process lead to construct of an asymmetric channel cross-section in meandering rivers. RCMM conceptualizes this physical process to build an empirical channel cross-section. The main steps of RCMM are presented below (Dey et al. 2019):

Stage 1: In this stage, the configuration of a river/channel (i.e., channel depth and width) goes into a non-dimensional space.

Stage 2: A power law function (Eq. 14) is used to locate the thalweg by utilizing the radius of curvature of the channel centerline.

$$t^* = \begin{cases} a(r^*)^{-b} - 0.5 & r^* > 2 \\ 0, & r^* \leq 2 \end{cases} \quad (14)$$

where t^* denotes the location of the river thalweg in the normalized coordinate system, and r^* is the normalized radius of curvature of the centerline segment. The coefficients of a and b are calibrated for the river based on the observed bathymetry data.

Stage 3: In this stage, a composite beta function is used to create a cross-sectional shape using three points from two left- and right-bank locations and the thalweg.

$$\widehat{\mathcal{Z}}^* = \{f(n^*|\alpha_1, \beta_1) + f(n^*|\alpha_2, \beta_2)\} \times k \quad (15)$$

where $\widehat{\mathcal{Z}}^*$ represents the depth predicte, $f(n^*|\alpha_1, \beta_1)$ and $f(n^*|\alpha_2, \beta_2)$ show the two beta functions, and k , α_1 , β_1 , α_2 and β_2 are coefficients depending on the thalweg location.

This leads to an asymmetric channel cross-section with the thalweg being closer to the outer bank in a meander.

2.4 Data Collection

To determine the Thalweg of a river using the proposed framework, it is first necessary to gather the topographic data of the river. Therefore, in the present study, the geographical position of the river was first identified on Google Earth, and then, a photo of the desired area was captured. In the Next step, the photo was uploaded into Global Mapper software and was georeferenced regarding the available coordinates. Afterward, the digital elevation model (DEM) file for the desired coordinates was downloaded and extracted to generate contour lines. Now it's time to digitize the map, which is done in Autocad Civil 3D software using the "Pline" command on the borders and any important lines in the river environment. Then, one takes the extracted contour lines to the Civil software and draws the desired lines, including the cross sections perpendicular to the left and right shore. In addition, the correlation of the points on the constructed surface can be calculated by using the "Point-divide obj" command on the desired points from drawn lines and interpolating them. Finally, the position of the concave line is determined using the points with the lowest height on cross sections.



Fig. 4 Location of the Shuibeicun reach (Liu et al. 2018)

3 Results and Implementation

3.1 Case Study I

The performance of the proposed approach using Adaptive Neuro-Fuzzy Inference System (ANFIS) and Artificial Neural Network (ANN) models for imitating the geometry of rivers was evaluated in two different case studies. The first case is the Shuibeicun reach in the Qinhe River in China (Fig. 4). Information on the river's coordinates of the X-, Y-, and Z-axes of its left, right banks, and thalweg is available.

Second to preparing the required data (i.e., normalization and segmentation for training and testing) and adjusting the parameters of ANFIS and ANN based on sensitivity analysis, researchers modeled the transversal and longitudinal sections of the river. The ANFIS and ANN adjustment values are presented in Table 1.

It is worth noting that the normalization of input data to AI-based models leads to data homogenization and increases prediction accuracy. In this study, Eq. (16) was used to normalize the collected data.

Table 1 Parameters setting for two methods

Model	Parameter	Value
ANFIS	Type	Sugeno-type
	Fuzzy Clustering	FCM
	MF type	Gaussian
	Number of fuzzy rules	12
	Maximum number of epochs in training	1000
ANN	Number of hidden layers	3
	Hidden layers' activation function	Hyperbolic tangent sigmoid
	Training algorithm	Levenberg-Marquardt
	Number of neurons in each hidden layer	16

$$x_n = \frac{x_{max} - x}{x_{max} - x_{min}} \quad (16)$$

where x_n is the normalized value of variable x , and x_{max} and x_{min} are the maximum and minimum values, respectively.

To evaluate the performance of ANFIS and ANN models and to examine their prediction accuracy, the common assessment evaluation criteria in the technical literature, including Root Mean Square Error (RMSE) was used. It is quite clear that the lower the RMSE value, the higher the model's prediction accuracy is.

$$RMSE = \sqrt{\frac{1}{n} \sum_{i=1}^n (y^i - \hat{y}^i)^2} \quad (17)$$

where y^i and \hat{y}^i are the observed and predicted values, respectively. Also, n indicated the number of samples. It should be noted that each of the coordinates, including X, Y, and Z, is modeled separately for the river's thalweg. For example, only the right and left X's have been used to predict the x-coordinates of thalweg. For Y and Z, only the left and right Y's and Z's have been used. Therefore, the parameter n in the above equation is the number of data related to each coordinate in each stage of modeling.

The data collected for the geometry of the studied rivers was modeled in the following combinations:

- (a) Train (50%), Test (50%).
- (b) Train (30%), Test (70%).

To eliminate the impacts of the selected data on the models' performance, we ran each model 10 times and randomly selected and modeled new data in each iteration. The best results for the first case study geometry by using ANFIS and ANN are reported in Table 2.

Table 2 The values of statistical indicators for the AI-based proposed models for predicting the thalweg of rivers

			Training	Test		
			RMSE(m)	R ²	RMSE(m)	R
Train= 50% Test= 50%	ANFIS	X	0.32	1.00	0.57	0.99
		Y	0.62	1.00	0.74	0.99
		Z	0.51	1.00	0.57	0.99
	ANN	X	5.07	1.00	11.38	0.99
		Y	3.88	1.00	10.47	0.99
		Z	5.44	0.5	5.23	0.67
Train= 30% Test= 70%	ANFIS	X	0.90	0.99	1.11	0.99
		Y	0.86	1.00	1.84	0.99
		Z	0.86	1.00	0.54	0.99
	ANN	X	4.48	1.00	8.16	0.99
		Y	4.9	1.00	4.7	0.99
		Z	5.36	0.50	5.47	0.61

As can be seen from Table 2, the two methods have had similar results, but based on the average evaluation criteria of RMSE, the accuracy of ANFIS estimation is generally higher than ANN. It can also be inferred from the table that both models (ANN and ANFIS) have higher accuracy through the first type of combination, i.e. Train 50%, Test 50%, than the combination of the second type, i.e. Train 30%, and Test 70%. It is noticeable that the predicted and measured data sets are presented in Appendix.

Figure 5 depicts a scheme of the predicted coordinates of the river thalweg using both models. This figure is related to the best results of each model in 10 runs. With the ANFIS model, in the test phase, the RMSE value of 0.32 for the X-axis, 0.62 for the Y-axis, and 0.51 for the Z-axis were selected out of all the runs.

Likewise, for the ANN model, the RMSE value of 4.48 for the X-axis, the RMSE of 4.9 for the Y-axis, and the RMSE of 5.36 for the Z-axis were selected out of all the runs.

As shown in Fig. 5, the modeled thalweg is in compliance with the measured thalweg. Figure 6 also shows the correlation between the predicted and measured values in both ANFIS and ANN models in the X-and Y-axes for all samples, including the training and testing phases. As can be noticed, the AI-based methods have a high accuracy in estimating the geometry of rivers owing to the point that the correlation coefficients of both models are equal to 0.99 and 0.98 for estimating the X-axis and Y-axis values, respectively.

To show the models' accuracy in estimating the coordinates of the thalweg based on AI methods, Fig. 7 shows the coverage of the estimated and observed points Z. As can be seen, the models have accurately estimated the thalweg height.

3.2 Case Study II

The second case study is a part of the Gaz River with a length of 22 km, located in Khuzestan Province, Iran. The Gaz is 55 km long and is considered the main drainage of the Gaz drainage basin, which originates from the Bashagard Mountains and flows into the Oman Sea. The topology information of the river used in this study was collected via the field survey (camera mapping) method. Figure 8 shows the Gaz basin and river.

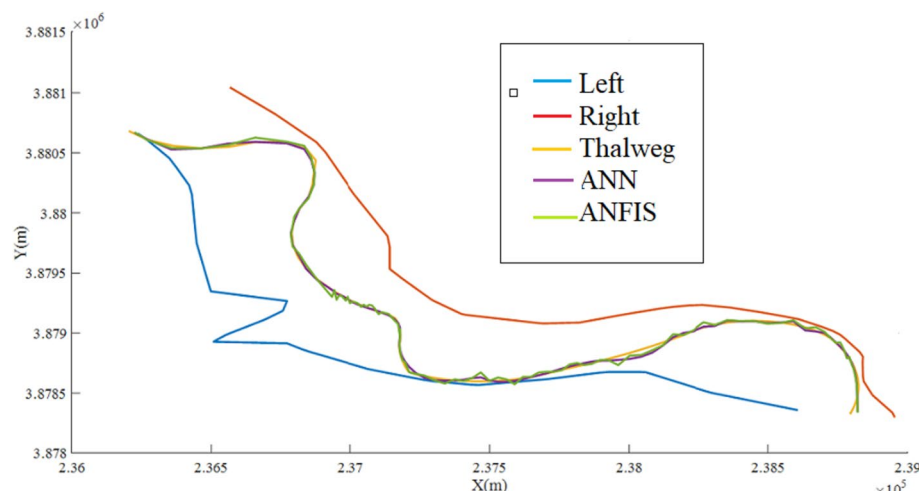


Fig. 5 Results of the predicted thalweg of China river using ANFIS and ANN

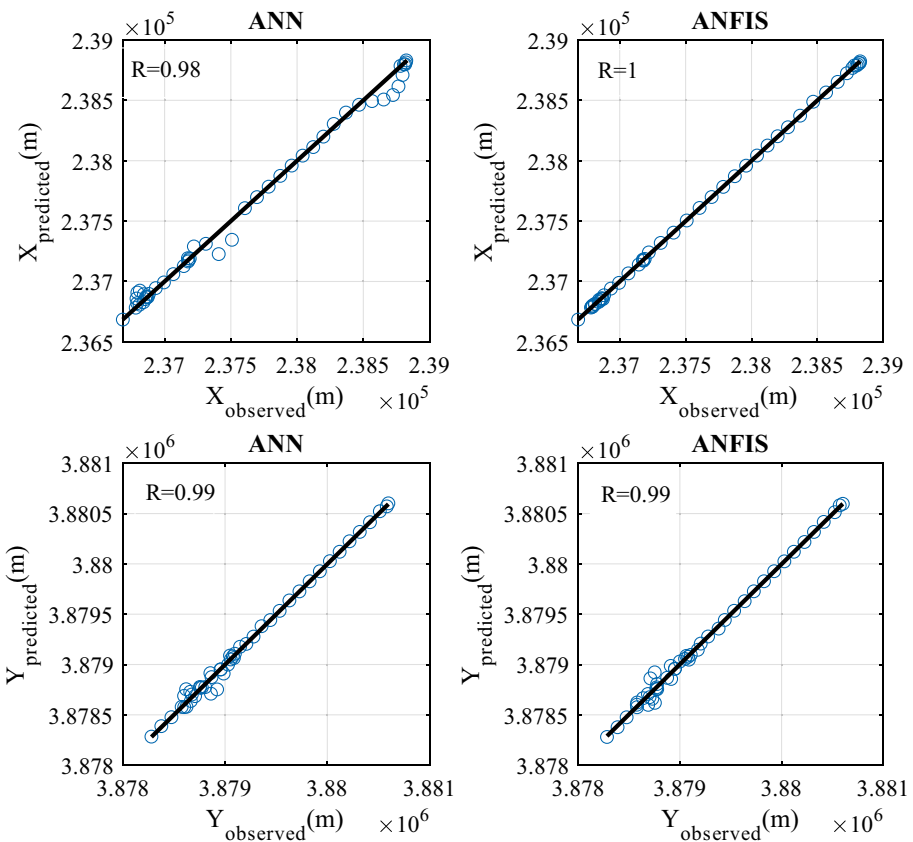


Fig. 6 The overall scatterplots of the proposed approach of ANFIS and ANN models (training and testing phases)

According to the steps followed to predict the thalweg of the Qinhe River, the thalweg of the Gaz was modeled using ANFIS and ANN. To this end, the same adjustment parameters used in the previous case study were applied in the case of Gaz River too.

Among 10 runs for ANFIS and ANN models. According to Table 3, both models have approximately the same accuracy. However, like the previous case study, the ANFIS model was generally more accurate and robust than the ANN. Moreover, the scheme of the thalweg obtained through the ANFIS and ANN models is illustrated in Fig. 9, for the purpose of showing the accuracy of the AI-based models.

Figure 9 illustrates that AI-based models simulate the geometry of rivers with high accuracy, which makes them a good alternative to field calculations and analytical models. Like the first case study, the Fig. 9 is related to the best results from each model in 10 runs.

With the ANFIS model, the RMSE value of 1.69 was selected for the X-axis ,and the RMSE values of 2 and 0.34 were picked for the Y- and the Z-axes, respectively. Similarly, with the ANN model, the RMSE values of 1.29, 1.38, and 0.52 were selected for the X-, Y-, and Z-axes out of 10 runs. Also, Fig. 8 shows the error of ANFIS and ANN models for the Z-axis of the thalweg.

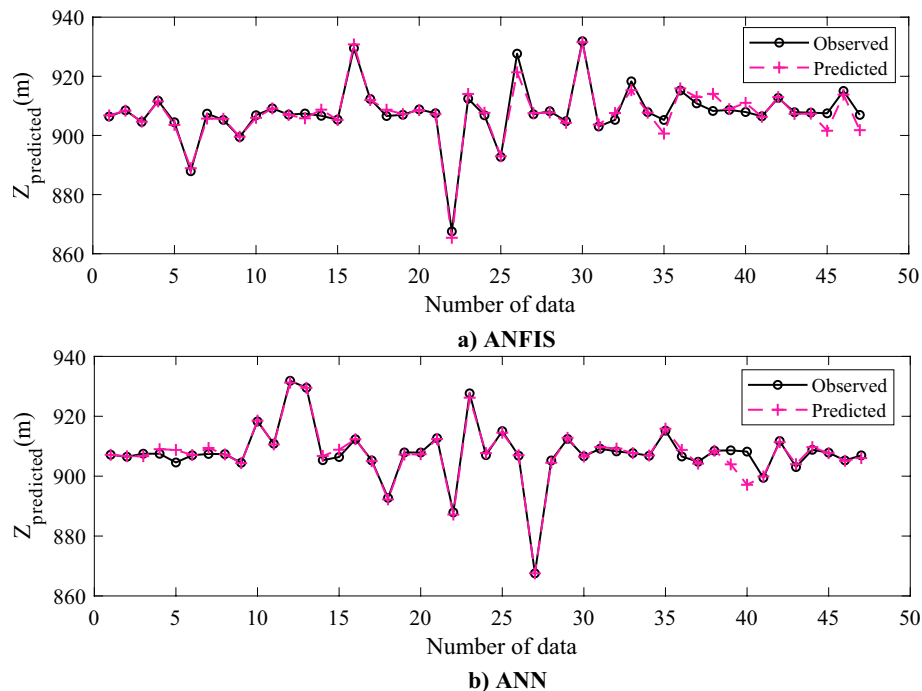


Fig. 7 The overall time series plots using the ANN and ANFIS models (training and testing performance)

Figures 10, 11, and 12 indicates that both models could estimate the coordinates of the thalweg with acceptable accuracy.

4 Comparative Performance

As mentioned in Section 2.3, RCMM is a conceptual model that has widely been used to estimate the thalweg of rivers. In this section, a comparative performance test of the AI-based framework against the RCMM model was carried out to show the efficiency of AI-based models. To this end, the geographic coordinates X and Y of the thalweg in the case study I were predicted based on the geographic coordinate of the right and left banks of the river using RCMM and the outcomes were compared with those of the two AI-based models.

Table 4 shows the values of statistical metrics for four models, including ANFIS, ANN, and RCMM models. According to this table, it is clear that the AI-based models outperform famous conceptual models in terms of statistical parameters (i.e., RMSE).

Moreover, the best model is the ANFIS, with $\text{RMSE}_X = 1.69 \text{ m}$, $\text{RMSE}_Y = 2 \text{ m}$, $\text{RMSE}_Z = 0.34 \text{ m}$. while the accuracy of the RCMM model is lower than two AI-based models.

Overall, it can be said that the numerical methods are not able to correctly simulate the thalweg of rivers since they usually face remarkable errors for measured points. However the AI-based models have been able to correctly simulate the thalweg of



Fig. 8 Location of the second case study

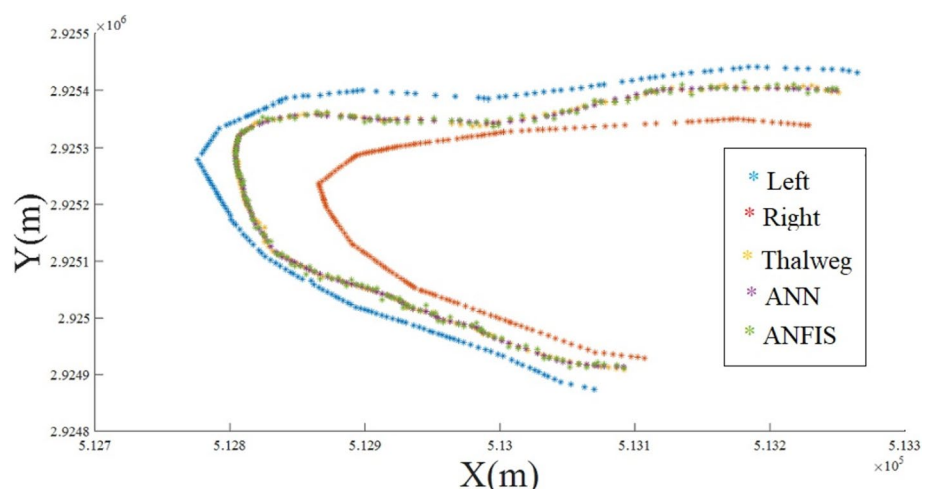
rivers, while the ANFIS method has had the most compatibility among them. Thus, it can be claimed that the ANFIS is the best model for the prediction of the thalweg of rivers. It can be concluded that by using AI methods, the thalweg of rivers can be accurately estimated with the lowest computational costs.

Table 3 The values of statistical indicators for the AI-based proposed models for the thalweg of rivers prediction in overall phases

		Training		Test	
		RMSE(m)	R ²	RMSE(m)	R
Train= 50% Test= 50%	ANFIS	X	1.69	0.97	3.76
		Y	2.00	0.99	3.1
		Z	0.34	0.37	0.41
	ANN	X	1.29	0.99	2.16
		Y	1.38	0.99	2.21
		Z	0.52	0.86	0.41
Train= 30% Test= 70%	ANFIS	X	1.79	0.99	2.19
		Y	2.00	0.99	2.67
		Z	0.25	0.51	0.64
	ANN	X	1.69	0.99	1.73
		Y	1.52	0.99	1.79
		Z	0.45	0.85	0.51

5 Discussion

In this study, the authors compared the performance of the AI-based models with that of a numerical model, namely RCMM, using data from two rivers in China and Iran. The results showed that AI-based models performed better than RCMM in terms of accuracy and efficiency. The ANFIS model also outperformed the ANN model, especially when data availability was limited. There are some questions such as why do the AI-based models work, why do they give better results than the analytical model, and what are the advantages and disadvantages of both types of models? It can be say that AI-based models are data-driven methods that learn from patterns and relationships

**Fig. 9** Results of the predicted thalweg of Gaz River using ANFIS and ANN

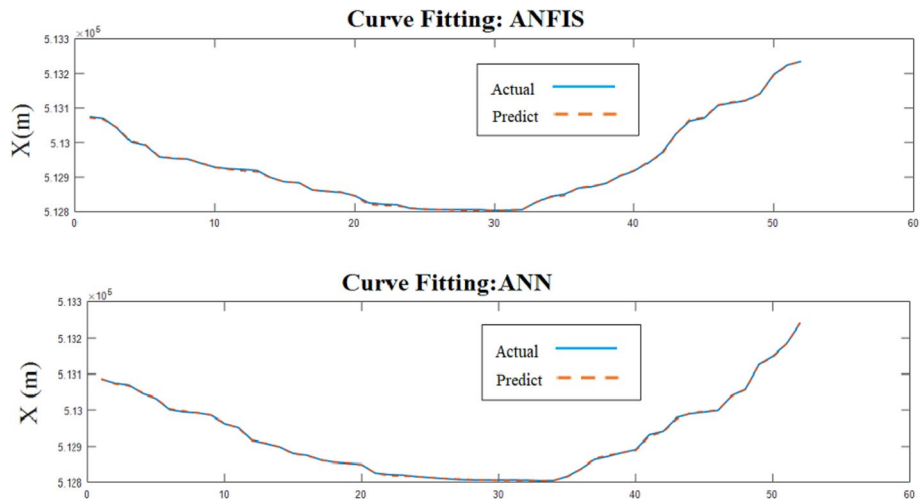


Fig. 10 The curve fitting of the proposed framework to predict the coordinate X using ANFIS and ANN for Gaz river

in the input and output data, without requiring any prior knowledge or assumptions about the system or the process that they are modeling. Therefore, they can adapt to different situations and conditions, as long as they have enough data to train and test them. Moreover, the results shown that that AI-based models are highly dependent on the quality and quantity of the data that they use, and that they may not be able to generalize to new cases or scenarios if the data is not representative of the system or the process that they are modeling. The results also showed that AI-based models are often considered as black-box methods that do not reveal how they make their predictions or what features they use to make their decisions.

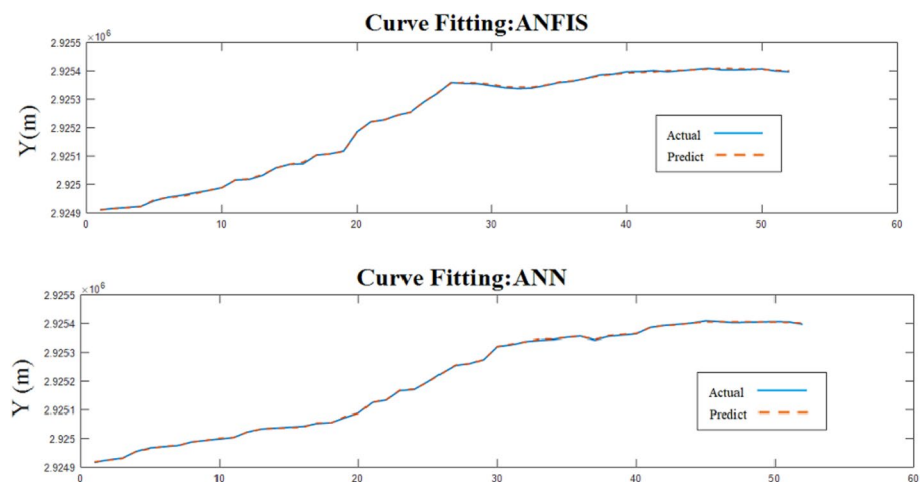


Fig. 11 The curve fitting of proposed framework to predict the normalized coordinate Y using ANFIS and ANN in Gaz river

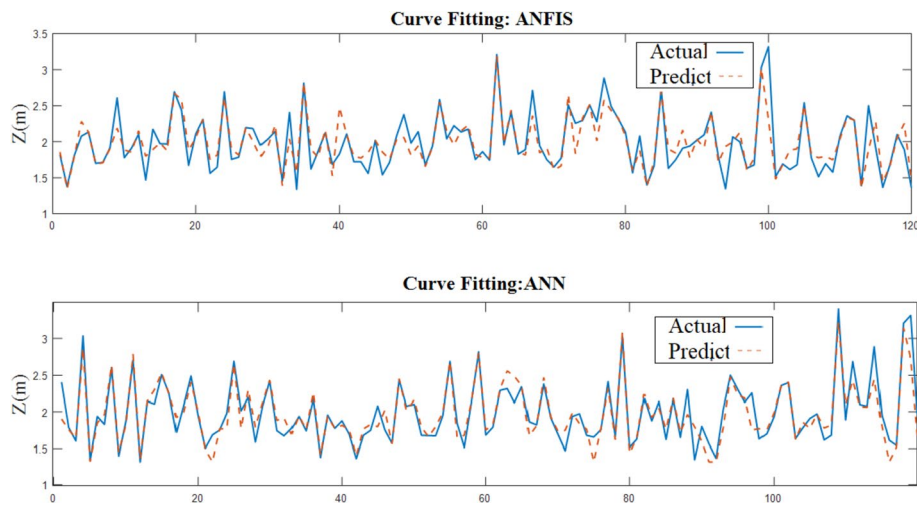


Fig. 12 The curve fitting of proposed framework to predict the normalized coordinate Z using ANFIS and ANN in Gaz river

Table 4 Comparison of prediction results of AI-based methods and RCMM

Methods			ANFIS	ANN	RCMM
Case I	X	RMSE (m)	0.32	5.08	43.2
	Y	RMSE (m)	0.62	3.88	59.6
	Z	RMSE (m)	0.51	5.55	4.04
Case II	X	RMSE (m)	1.69	1.29	48.9
	Y	RMSE (m)	2	1.38	24.67
	Z	RMSE (m)	0.34	0.27	0.9

6 Conclusion

Given the importance of rivers' topography in their hydrodynamic modeling, this study proposed a new approach based on ANFIS and ANN methods for modeling and estimating a river's thalweg. The efficiency of these models was evaluated in two cases, the Qinhe River and the Gaz River in China and Iran, respectively. Also, the stability of the models was evaluated, and the errors caused by the selection of training and testing data were eliminated by replicating the modeling 10 times by selecting various data. The modeling results for the first case, which had a smaller database, showed that ANN had better accuracy than the ANFIS in modeling the river's thalweg. Also, for the second case, which had a large database, the ANFIS simulated the river coordinates more accurately. In general, comparing these two methods shows that the ANFIS model is more robust than the ANN model because the values of statistical parameters of the model have been much lower than ANN. Nevertheless, both models can be used as effective tools for estimating the thalweg of rivers. Moreover, comparing results obtained from the AI-based models to the RCMM model showed that the ANN yielded the lowest prediction error. Since determining the weight and bias values in ANN and ANFIS parameters has a significant role in the accuracy of

prediction, it is suggested to use a combination of meta-heuristic optimization methods to determine these parameters in future studies. It is also recommended to present a robust model for estimating the topography of rivers by combining an uncertainty-based model such as MCS, ANFIS, and ANN models, taking into account the effect of existing uncertainties. Also, in order to better evaluate the effectiveness of artificial intelligence models, it is recommended that the models be trained using data from 10 rivers and then applied to another river to determine their accuracy.

Appendix

Case study I:

Left			Talweg			Right		
x	y	z	X	Y	Z	X	Y	Z
238607.47	3878357.49	824.23	238794.24	3878324.99	801.10	238954.52	3878297.10	834.39
238591.26	3878365.05	823.81	238802.93	3878359.96	805.34	238946.04	3878335.94	834.99
238575.04	3878372.61	824.00	238810.18	3878395.26	811.82	238928.31	3878372.47	837.59
238558.83	3878380.18	824.20	238815.96	3878430.82	822.03	238910.57	3878409.00	840.91
238542.62	3878387.74	824.79	238820.26	3878466.60	830.83	238892.83	3878445.53	841.80
238526.41	3878395.30	826.04	238823.08	3878502.52	836.73	238875.10	3878482.06	844.03
238510.19	3878402.86	826.64	238824.41	3878538.53	840.60	238863.97	3878521.07	843.98
238493.98	3878410.43	826.67	238824.25	3878574.56	842.98	238853.43	3878560.28	846.80
238477.77	3878417.99	826.48	238822.60	3878610.56	844.76	238842.88	3878599.50	849.88
238461.56	3878425.55	824.58	238819.46	3878646.46	841.70	238840.69	3878639.86	849.37
238445.34	3878433.11	822.69	238814.84	3878682.19	835.63	238840.27	3878680.47	843.39
238429.13	3878440.67	822.93	238808.74	3878717.71	831.82	238839.85	3878721.08	837.03
238412.92	3878448.24	823.58	238801.19	3878752.94	828.32	238839.43	3878761.69	831.91
238396.71	3878455.80	824.43	238792.18	3878787.83	823.13	238840.73	3878802.27	830.24
238380.49	3878463.36	825.51	238781.73	3878822.31	819.69	238829.53	3878840.23	830.97
238364.28	3878470.92	826.53	238769.87	3878856.34	819.67	238812.24	3878876.98	833.84
238348.07	3878478.48	827.18	238756.61	3878889.84	820.36	238794.96	3878913.73	838.47
238331.85	3878486.05	827.83	238741.98	3878922.77	821.73	238777.68	3878950.48	842.58
238315.64	3878493.61	827.03	238726.00	3878955.07	825.47	238758.63	3878986.10	850.55
238299.43	3878501.17	825.75	238704.56	3878983.83	828.33	238732.70	3879017.36	850.62
238281.57	3878512.31	824.14	238670.82	3879018.47	831.33	238693.46	3879051.44	852.56
238264.40	3878524.47	822.34	238632.37	3879047.82	832.54	238651.97	3879083.20	854.59
238247.36	3878536.83	820.96	238590.06	3879071.25	826.39	238610.48	3879114.96	849.58
238230.33	3878549.18	821.63	238544.79	3879088.25	824.52	238563.14	3879136.52	838.86
238213.29	3878561.54	819.38	238497.52	3879098.47	822.85	238514.79	3879156.33	837.01
238196.25	3878573.90	821.34	238449.26	3879101.68	823.55	238466.34	3879175.88	842.96
238179.21	3878586.25	823.77	238401.05	3879097.82	824.95	238417.18	3879193.56	853.34
238162.17	3878598.61	824.83	238353.92	3879086.97	823.85	238367.99	3879211.16	861.32
238145.14	3878610.96	824.28	238308.88	3879069.36	824.04	238317.02	3879222.65	857.35
238128.10	3878623.32	823.08	238266.88	3879045.37	829.22	238266.00	3879233.45	851.22
238111.06	3878635.68	821.66	238228.84	3879015.51	829.32	238213.90	3879229.61	844.74
238094.02	3878648.03	821.09	238193.73	3878982.23	827.29	238162.90	3879219.25	837.94

Left			Talweg			Right		
x	y	z	X	Y	Z	X	Y	Z
238076.98	3878660.39	821.07	238156.93	3878950.78	824.65	238112.80	3879204.57	837.40
238059.95	3878672.74	821.26	238119.37	3878920.25	822.00	238063.99	3879185.93	835.66
238039.72	3878675.23	820.07	238081.07	3878890.66	821.10	238015.18	3879167.30	835.38
238018.67	3878675.16	819.14	238042.05	3878862.02	820.62	237966.66	3879147.95	836.37
237997.63	3878675.10	818.60	238002.33	3878834.34	820.78	237918.51	3879127.65	836.08
237976.58	3878675.03	818.14	237961.95	3878807.66	821.93	237870.37	3879107.35	830.96
237955.53	3878674.96	817.59	237920.92	3878781.97	821.43	237822.22	3879087.06	825.83
237923.82	3878674.87	818.10	237894.31	3878766.06	821.09	237806.35	3879086.11	825.03
237892.90	3878669.26	819.40	237867.21	3878750.99	820.12	237790.48	3879085.16	824.48
237862.42	3878660.48	819.57	237839.90	3878736.31	822.96	237774.61	3879084.21	825.34
237831.95	3878651.69	819.04	237812.58	3878721.62	821.44	237758.74	3879083.26	826.19
237801.48	3878642.91	821.33	237785.27	3878706.94	821.00	237742.88	3879082.30	826.12
237771.01	3878634.12	822.15	237757.96	3878692.25	821.55	237727.01	3879081.35	825.90
237740.54	3878625.34	821.66	237730.65	3878677.57	821.37	237711.14	3879080.40	825.53
237710.07	3878616.55	820.28	237703.34	3878662.89	819.11	237695.27	3879079.45	824.33
237679.01	3878610.16	819.38	237676.03	3878648.20	817.55	237679.66	3879081.18	823.02
237647.91	3878603.99	818.52	237648.10	3878634.77	819.78	237664.28	3879085.22	822.33
237616.80	3878597.81	818.82	237619.20	3878623.55	820.24	237648.91	3879089.26	821.70
237585.70	3878591.63	819.16	237589.62	3878614.26	820.62	237633.53	3879093.30	821.48
237554.59	3878585.46	819.15	237559.49	3878606.96	820.43	237618.16	3879097.34	822.18
237523.49	3878579.28	819.36	237528.94	3878601.66	819.99	237602.78	3879101.38	823.03
237492.38	3878573.10	818.38	237498.11	3878598.39	819.20	237587.40	3879105.42	825.43
237461.28	3878566.93	817.23	237467.13	3878597.16	817.30	237572.03	3879109.46	827.76
237430.25	3878570.56	817.92	237436.14	3878597.99	816.44	237556.65	3879113.51	828.62
237399.24	3878577.21	819.23	237405.27	3878600.86	817.22	237541.27	3879117.55	827.55
237368.23	3878583.87	819.99	237374.65	3878605.76	817.84	237525.90	3879121.59	826.06
237332.64	3878591.16	820.11	237338.48	3878614.29	818.56	237509.81	3879125.81	824.10
237297.04	3878598.46	819.35	237303.10	3878625.66	819.00	237493.72	3879130.04	822.12
237262.88	3878610.23	818.78	237268.73	3878639.80	818.28	237477.64	3879134.27	821.35
237229.73	3878625.11	818.64	237235.59	3878656.61	818.44	237461.55	3879138.50	821.46
237196.58	3878640.00	821.03	237209.04	3878679.89	819.84	237445.46	3879142.73	821.28
237163.43	3878654.88	823.81	237199.14	3878715.72	820.62	237429.37	3879146.95	821.27
237130.28	3878669.77	825.22	237190.98	3878751.98	822.19	237413.29	3879151.18	821.38
237097.13	3878684.65	826.16	237184.61	3878788.60	820.98	237399.20	3879158.70	821.27
237064.32	3878700.15	831.14	237180.01	3878825.48	818.52	237388.02	3879171.02	821.30
237034.21	3878720.50	827.97	237177.22	3878862.55	812.35	237376.84	3879183.34	821.11
237004.10	3878740.84	826.10	237176.40	3878899.69	804.77	237365.66	3879195.65	821.18
236973.99	3878761.19	825.95	237180.03	3878936.68	802.28	237354.48	3879207.97	821.47
236943.88	3878781.54	825.94	237181.33	3878973.83	803.50	237343.30	3879220.29	822.13
236913.78	3878801.88	825.38	237180.30	3879010.98	809.14	237332.12	3879232.60	822.95
236883.67	3878822.23	826.40	237176.96	3879048.00	812.83	237320.94	3879244.92	823.31
236853.56	3878842.57	829.38	237171.30	3879084.73	815.18	237309.76	3879257.24	823.66
236824.95	3878864.82	830.15	237163.35	3879121.04	817.76	237298.58	3879269.55	824.01
236798.09	3878889.30	827.93	237141.86	3879148.46	819.68	237289.07	3879283.11	824.10

Left			Talweg			Right		
x	y	z	X	Y	Z	X	Y	Z
236771.23	3878913.78	825.69	237111.77	3879170.27	822.40	237280.53	3879297.38	824.78
236756.40	3878927.30	825.39	237101.09	3879178.52	823.61	237275.60	3879305.63	825.47
236741.56	3878940.81	824.82	237090.55	3879186.95	825.21	237270.67	3879313.88	825.56
236726.73	3878954.33	824.92	237080.15	3879195.55	826.80	237265.74	3879322.13	825.57
236711.89	3878967.85	824.84	237069.90	3879204.32	828.37	237260.80	3879330.37	825.70
236697.06	3878981.37	824.55	237059.79	3879213.25	828.82	237255.87	3879338.62	825.22
236682.22	3878994.89	824.40	237049.83	3879222.35	827.84	237250.94	3879346.87	825.73
236667.39	3879008.41	824.89	237040.02	3879231.62	826.86	237246.00	3879355.12	826.15
236652.56	3879021.93	825.38	237030.36	3879241.04	825.86	237241.07	3879363.37	825.29
236637.72	3879035.44	824.02	237020.86	3879250.63	824.66	237236.14	3879371.61	824.71
236622.89	3879048.96	822.32	237011.52	3879260.36	823.64	237231.20	3879379.86	824.28
236608.05	3879062.48	820.90	237002.34	3879270.25	822.64	237226.27	3879388.11	823.85
236593.22	3879076.00	821.36	236993.32	3879280.29	821.64	237221.34	3879396.36	823.42
236578.39	3879089.52	821.80	236984.47	3879290.48	820.80	237216.40	3879404.61	822.83
236563.55	3879103.04	821.72	236975.79	3879300.81	820.04	237211.47	3879412.85	822.81
236550.11	3879117.74	820.98	236967.28	3879311.28	819.27	237206.54	3879421.10	823.03
236539.22	3879134.59	820.25	236958.95	3879321.89	818.49	237201.61	3879429.35	823.25
236528.33	3879151.45	820.58	236950.79	3879332.64	817.83	237196.67	3879437.60	823.46
236517.44	3879168.31	820.90	236942.80	3879343.52	817.67	237191.74	3879445.85	823.51
236508.43	3879185.85	821.63	236935.00	3879354.53	817.36	237186.81	3879454.09	823.30
236498.28	3879266.27	821.23	236881.97	3879441.80	817.82	237142.55	3879533.61	822.40
236488.14	3879346.69	821.90	236840.20	3879534.98	816.35	237142.55	3879625.36	818.61
236477.99	3879427.11	822.59	236810.33	3879632.64	820.78	237142.43	3879717.10	826.62
236467.85	3879507.53	823.00	236792.84	3879733.25	819.39	237134.65	3879807.80	826.66
236457.70	3879587.95	824.74	236787.98	3879835.26	819.43	237104.64	3879894.50	824.00
236447.55	3879668.37	819.28	236795.84	3879937.07	819.85	237074.64	3879981.20	820.13
236443.84	3879749.32	815.33	236816.30	3880037.12	823.10	237044.63	3880067.90	825.16
236440.53	3879830.31	823.90	236849.03	3880133.86	821.11	237014.62	3880154.60	824.49
236437.22	3879911.30	824.47	236861.82	3880234.23	815.90	236987.30	3880242.17	816.60
236433.90	3879992.29	819.77	236867.49	3880336.26	830.57	236961.15	3880330.11	824.15
236430.59	3880073.28	813.44	236873.95	3880438.17	837.13	236935.01	3880418.05	829.97
236420.57	3880153.12	817.91	236840.62	3880533.06	827.55	236908.86	3880505.99	827.90
236396.78	3880230.60	817.30	236758.50	3880591.11	814.17	236875.72	3880590.77	834.95
236372.98	3880308.09	819.45	236657.93	3880590.86	818.88	236826.87	3880668.43	827.37
236349.18	3880385.57	826.33	236564.28	3880550.92	825.70	236778.02	3880746.08	833.31
236312.03	3880457.54	827.75	236463.19	3880539.14	821.00	236728.87	3880823.54	831.76
236274.20	3880529.23	820.84	236363.34	3880558.84	824.41	236674.79	3880897.65	835.14
236236.37	3880600.92	820.39	236274.29	3880608.12	823.53	236620.71	3880971.77	836.65
236184.88	3880662.49	822.60	236204.57	3880682.26	823.44	236566.63	3881045.88	830.64

Cas study II:

Left			Talweg			Right		
x	y	z	x	y	z	x	y	z
513069.80	2924874.00	6.61	513092.00	2924909.00	1.97	513107.10	2924929.00	5.73
513062.69	2924878.00	6.70	513086.31	2924911.00	2.02	513102.05	2924931.00	5.72
513052.58	2924883.00	6.82	513080.47	2924913.00	2.08	513097.20	2924932.00	5.72
513045.00	2924887.00	6.91	513074.84	2924914.00	2.13	513089.98	2924934.00	5.71
513040.50	2924892.00	7.04	513070.00	2924916.00	2.18	513083.80	2924936.00	5.70
513035.60	2924897.00	7.18	513064.31	2924917.00	1.93	513077.14	2924938.00	5.69
513032.68	2924900.00	7.22	513057.90	2924919.00	1.66	513070.50	2924939.00	5.68
513028.79	2924905.00	7.26	513051.65	2924923.00	2.08	513065.25	2924944.00	5.69
513025.80	2924908.00	7.30	513046.52	2924926.00	2.41	513059.50	2924949.00	5.69
513022.25	2924912.00	7.24	513041.70	2924929.00	2.73	513052.84	2924954.00	5.70
513016.70	2924917.00	7.15	513037.10	2924932.00	3.03	513047.30	2924959.00	5.70
513012.95	2924921.00	7.01	513032.26	2924935.00	2.54	513041.10	2924964.00	5.71
513008.71	2924926.00	6.86	513027.99	2924938.00	2.11	513035.90	2924969.00	5.71
513002.30	2924933.00	6.64	513020.50	2924943.00	1.35	513030.06	2924974.00	5.72
512998.58	2924936.00	6.65	513013.89	2924949.00	2.41	513024.00	2924979.00	5.72
512993.31	2924941.00	6.68	513007.70	2924955.00	3.40	513019.97	2924982.00	5.72
512989.30	2924944.00	6.70	513000.99	2924962.00	2.61	513015.70	2924986.00	5.72
512983.97	2924948.00	6.67	512994.90	2924968.00	1.89	513011.64	2924989.00	5.73
512978.24	2924953.00	6.63	512992.19	2924971.00	1.86	513008.13	2924992.00	5.74
512973.10	2924957.00	6.59	512987.51	2924972.00	2.28	513006.90	2924993.00	5.74
512969.19	2924960.00	6.60	512986.27	2924976.00	1.79	513003.80	2924996.00	5.75
512966.01	2924963.00	6.60	512983.40	2924979.00	1.75	512999.79	2924999.00	5.72
512963.19	2924965.00	6.60	512980.99	2924983.00	1.91	512996.99	2925002.00	5.71
512960.36	2924967.00	6.60	512979.10	2924986.00	2.03	512993.19	2925005.00	5.69
512957.27	2924970.00	6.61	512973.01	2924989.00	1.95	512988.20	2925009.00	5.66
512954.40	2924972.00	6.61	512967.30	2924991.00	1.88	512985.01	2925012.00	5.64
512950.38	2924975.00	6.61	512962.82	2924994.00	1.87	512979.95	2925016.00	5.61
512947.99	2924977.00	6.61	512958.70	2924996.00	1.86	512974.50	2925021.00	5.58
512943.78	2924981.00	6.62	512954.00	2924999.00	1.94	512968.94	2925026.00	5.60
512940.20	2924984.00	6.62	512952.33	2925004.00	1.72	512965.94	2925028.00	5.61
512936.00	2924987.00	6.58	512950.40	2925010.00	1.47	512962.90	2925031.00	5.61
512930.35	2924992.00	6.53	512944.60	2925012.00	1.65	512960.40	2925033.00	5.62
512927.51	2924994.00	6.51	512939.77	2925014.00	1.78	512956.79	2925036.00	5.64
512924.60	2924996.00	6.48	512935.40	2925016.00	1.89	512952.40	2925040.00	5.65
512920.41	2924999.00	6.44	512930.70	2925018.00	2.01	512950.24	2925042.00	5.66
512916.12	2925002.00	6.41	512932.10	2925023.00	1.98	512947.99	2925044.00	5.67
512912.50	2925005.00	6.37	512928.90	2925027.00	1.88	512945.17	2925046.00	5.68
512908.42	2925008.00	6.35	512926.52	2925030.00	1.81	512942.51	2925048.00	5.69
512905.10	2925011.00	6.33	512924.42	2925032.00	1.74	512941.24	2925049.00	5.70
512902.34	2925013.00	6.33	512922.60	2925034.00	1.68	512937.10	2925053.00	5.71
512899.81	2925015.00	6.33	512919.34	2925037.00	1.70	512935.46	2925056.00	5.70
512896.70	2925017.00	6.33	512916.90	2925040.00	1.71	512934.17	2925058.00	5.70

Left			Talweg			Right		
x	y	z	x	y	z	x	y	z
512893.20	2925019.00	6.32	512912.50	2925043.00	1.70	512932.69	2925060.00	5.69
512889.65	2925024.00	6.30	512907.90	2925047.00	1.68	512931.01	2925063.00	5.68
512887.30	2925027.00	6.29	512904.01	2925050.00	1.68	512929.20	2925066.00	5.67
512883.79	2925031.00	6.29	512901.75	2925051.00	1.68	512926.68	2925070.00	5.65
512880.70	2925035.00	6.30	512898.75	2925053.00	1.68	512923.55	2925075.00	5.63
512878.33	2925038.00	6.30	512895.20	2925056.00	1.68	512920.39	2925080.00	5.61
512875.40	2925042.00	6.32	512890.66	2925059.00	1.78	512917.90	2925084.00	5.60
512872.17	2925046.00	6.31	512886.20	2925061.00	1.88	512915.48	2925088.00	5.58
512868.71	2925050.00	6.30	512883.53	2925065.00	2.04	512913.70	2925091.00	5.57
512865.90	2925054.00	6.29	512880.50	2925069.00	2.22	512911.62	2925095.00	5.55
512862.24	2925059.00	6.26	512875.15	2925071.00	2.11	512908.87	2925099.00	5.52
512860.20	2925066.00	6.00	512868.90	2925073.00	1.97	512906.70	2925103.00	5.50
512853.57	2925069.00	6.21	512865.53	2925077.00	2.44	512903.89	2925108.00	5.50
512850.40	2925073.00	6.21	512862.30	2925081.00	2.88	512901.45	2925112.00	5.51
512846.98	2925078.00	6.20	512858.87	2925085.00	2.69	512899.40	2925115.00	5.51
512844.80	2925081.00	6.20	512855.34	2925089.00	2.49	512897.68	2925118.00	5.51
512841.29	2925086.00	6.19	512852.70	2925092.00	2.34	512894.75	2925123.00	5.52
512837.17	2925092.00	6.18	512849.58	2925096.00	2.20	512891.80	2925128.00	5.52
512833.90	2925097.00	6.18	512846.15	2925100.00	2.04	512890.40	2925130.00	5.52
512830.03	2925102.00	6.17	512843.30	2925104.00	1.91	512888.69	2925136.00	5.50
512826.10	2925108.00	6.15	512839.96	2925108.00	2.12	512886.80	2925142.00	5.48
512823.44	2925114.00	6.12	512836.00	2925113.00	2.38	512884.90	2925149.00	5.46
512821.50	2925119.00	6.10	512831.50	2925118.00	1.73	512882.69	2925156.00	5.45
512817.22	2925129.00	5.65	512828.60	2925126.00	1.94	512880.90	2925162.00	5.43
512814.50	2925136.00	5.37	512825.60	2925134.00	2.08	512878.96	2925168.00	5.42
512812.19	2925142.00	4.81	512825.60	2925142.00	1.94	512877.96	2925172.00	5.42
512809.90	2925147.00	4.25	512825.60	2925148.00	1.82	512876.70	2925176.00	5.41
512807.30	2925156.00	3.93	512825.60	2925159.00	1.63	512875.78	2925179.00	5.41
512804.35	2925164.00	4.02	512821.60	2925167.00	1.67	512874.52	2925184.00	5.40
512802.69	2925168.00	4.07	512819.84	2925171.00	1.69	512873.20	2925189.00	5.39
512800.80	2925173.00	4.13	512817.50	2925176.00	1.71	512871.40	2925195.00	5.38
512800.30	2925181.00	4.29	512815.50	2925186.00	2.10	512870.99	2925198.00	5.38
512798.65	2925187.00	4.45	512813.81	2925193.00	2.41	512870.47	2925202.00	5.37
512797.11	2925193.00	4.61	512812.70	2925198.00	2.61	512869.70	2925207.00	5.37
512795.70	2925198.00	4.75	512812.09	2925201.00	2.52	512869.47	2925208.73	5.37
512794.45	2925203.00	4.89	512810.70	2925207.00	2.30	512869.08	2925212.00	5.36
512792.90	2925209.00	5.07	512809.95	2925215.00	2.51	512868.60	2925216.00	5.36
512791.91	2925213.00	5.19	512809.30	2925221.00	2.69	512867.90	2925221.00	5.36
512790.79	2925218.00	5.32	512808.61	2925228.00	2.56	512867.10	2925226.00	5.35
512789.90	2925222.00	5.42	512807.94	2925234.00	2.42	512866.46	2925231.00	5.37
512788.52	2925228.00	5.50	512807.40	2925239.00	2.31	512866.11	2925234.00	5.38
512787.18	2925233.00	5.58	512806.77	2925245.00	2.02	512865.70	2925237.00	5.39
512785.85	2925238.00	5.65	512806.20	2925251.00	1.75	512868.30	2925241.00	5.39
512784.74	2925243.00	5.72	512805.80	2925255.00	1.58	512871.00	2925246.00	5.39

Left			Talweg			Right		
x	y	z	x	y	z	x	y	z
512783.70	2925247.00	5.78	512805.80	2925261.00	1.77	512873.19	2925250.00	5.35
512782.25	2925253.00	5.82	512805.80	2925267.00	1.95	512875.20	2925254.00	5.32
512780.80	2925259.00	5.85	512805.80	2925271.00	2.08	512877.81	2925259.00	5.28
512779.23	2925266.00	5.89	512805.80	2925275.00	2.18	512880.54	2925264.00	5.23
512777.63	2925272.00	5.94	512805.50	2925277.00	2.29	512882.80	2925268.00	5.19
512776.10	2925279.00	5.97	512804.20	2925285.00	1.83	512885.90	2925273.00	5.15
512779.30	2925290.00	5.98	512803.30	2925291.00	1.84	512888.07	2925277.00	5.11
512781.01	2925296.00	5.98	512803.67	2925296.00	1.82	512890.00	2925280.00	5.08
512782.69	2925302.00	5.99	512804.00	2925300.00	1.80	512891.51	2925283.00	5.06
512784.10	2925307.00	5.99	512804.28	2925303.00	1.77	512892.92	2925285.00	5.03
512785.96	2925313.00	6.02	512804.73	2925307.00	1.72	512893.80	2925287.00	5.01
512787.91	2925320.00	6.06	512805.20	2925312.00	1.67	512896.11	2925288.00	5.02
512789.70	2925326.00	6.09	512805.75	2925316.00	1.63	512898.74	2925290.00	5.02
512792.00	2925334.00	5.96	512806.30	2925321.00	1.58	512900.99	2925291.00	5.03
512797.33	2925340.00	5.95	512808.36	2925325.00	2.10	512903.07	2925292.00	5.03
512800.07	2925343.00	5.94	512809.95	2925327.00	2.50	512905.30	2925293.00	5.04
512803.42	2925346.00	5.94	512813.20	2925333.00	3.32	512907.28	2925294.00	5.04
512806.90	2925350.00	5.93	512816.20	2925338.00	2.71	512910.20	2925295.00	5.05
512811.86	2925355.00	5.95	512818.20	2925342.00	2.30	512912.11	2925296.00	5.05
512813.50	2925357.00	5.96	512820.10	2925345.00	1.92	512913.64	2925297.00	5.05
512815.94	2925359.00	5.97	512827.05	2925348.00	2.00	512916.05	2925298.00	5.04
512818.08	2925362.00	5.97	512832.80	2925350.00	2.07	512917.19	2925299.00	5.04
512821.20	2925365.00	5.98	512837.57	2925352.00	2.21	512919.90	2925300.00	5.04
512825.20	2925369.00	5.99	512843.70	2925354.00	2.39	512921.89	2925301.00	5.03
512827.17	2925371.00	6.00	512850.37	2925357.00	2.03	512923.81	2925302.00	5.03
512831.90	2925376.00	6.01	512854.70	2925359.00	1.79	512926.60	2925303.00	5.02
512836.37	2925381.00	6.01	512863.40	2925360.00	1.74	512930.03	2925304.00	5.01
512838.44	2925383.00	6.02	512867.71	2925360.00	1.79	512933.00	2925305.00	5.00
512841.50	2925386.00	6.02	512872.10	2925361.00	1.83	512935.82	2925306.32	4.99
512848.10	2925388.00	6.04	512882.50	2925358.00	1.92	512937.70	2925307.00	4.98
512854.30	2925390.00	6.03	512890.90	2925356.00	2.10	512940.98	2925308.00	4.97
512857.80	2925390.00	6.03	512892.90	2925355.00	2.14	512944.85	2925309.00	4.96
512866.90	2925391.00	6.00	512898.50	2925353.00	2.17	512947.70	2925310.00	4.95
512873.40	2925394.00	6.01	512903.10	2925352.00	2.14	512953.90	2925312.00	4.67
512881.05	2925396.00	6.00	512911.40	2925349.00	2.09	512958.00	2925313.00	4.49
512886.60	2925397.00	5.99	512913.30	2925348.00	2.02	512961.70	2925314.00	4.32
512891.00	2925398.00	6.00	512917.60	2925349.00	2.13	512968.35	2925316.00	3.95
512894.44	2925399.00	6.01	512922.60	2925351.00	2.14	512972.40	2925318.00	3.73
512898.20	2925400.00	6.02	512931.80	2925354.00	2.25	512975.82	2925319.00	3.54
512908.40	2925398.00	6.13	512941.10	2925351.00	2.40	512979.17	2925320.00	3.35
512920.14	2925396.00	6.10	512951.30	2925348.00	2.58	512983.45	2925321.00	3.11
512931.22	2925395.00	6.08	512964.20	2925343.00	2.69	512986.40	2925322.00	2.95
512937.30	2925394.00	6.07	512970.90	2925341.00	2.51	512988.61	2925323.00	2.91
512952.20	2925391.00	6.10	512979.70	2925338.00	2.36	512992.21	2925324.00	2.85

Left			Talweg			Right		
x	y	z	x	y	z	x	y	z
512966.90	2925389.00	6.16	512984.90	2925339.00	1.94	512995.50	2925325.00	2.79
512984.11	2925387.00	6.16	512990.00	2925340.00	1.70	512997.39	2925326.00	2.84
512988.10	2925386.00	6.16	512994.50	2925343.00	1.50	513000.48	2925327.00	2.93
512991.50	2925385.00	6.17	512998.90	2925346.00	1.32	513002.80	2925328.00	2.99
512999.48	2925388.00	6.15	513008.20	2925349.00	1.57	513008.10	2925329.00	3.13
513004.20	2925389.00	6.14	513017.54	2925352.00	1.97	513016.19	2925330.00	3.39
513011.91	2925391.00	6.15	513025.10	2925355.00	2.30	513021.70	2925331.00	3.57
513019.68	2925393.00	6.15	513033.30	2925359.00	2.81	513028.12	2925332.00	3.78
513025.80	2925395.00	6.16	513040.40	2925362.00	3.03	513031.70	2925332.00	3.90
513032.46	2925397.00	6.18	513046.30	2925364.00	3.21	513036.98	2925333.00	4.07
513039.78	2925399.00	6.20	513053.10	2925367.00	1.36	513041.29	2925333.00	4.21
513045.20	2925400.00	6.21	513057.80	2925370.00	1.51	513048.20	2925334.00	4.43
513053.37	2925402.00	6.21	513062.00	2925374.00	1.65	513055.40	2925335.00	4.67
513060.20	2925404.00	6.21	513070.90	2925380.00	1.94	513062.70	2925336.00	4.90
513067.62	2925407.00	6.19	513077.90	2925380.00	1.75	513069.39	2925337.00	5.01
513073.39	2925409.00	6.17	513084.80	2925380.00	1.97	513078.00	2925338.00	5.15
513077.00	2925410.00	6.16	513095.10	2925386.00	1.56	513085.06	2925339.00	5.17
513090.50	2925415.00	6.12	513101.30	2925389.00	1.51	513092.60	2925340.00	5.20
513097.80	2925417.00	6.04	513107.72	2925393.00	1.60	513107.60	2925342.00	5.10
513104.73	2925420.00	5.96	513112.90	2925397.00	1.67	513115.70	2925343.00	5.08
513110.89	2925422.00	5.89	513115.10	2925398.00	1.62	513129.80	2925344.00	5.06
513115.20	2925423.00	5.85	513121.10	2925401.00	1.96	513139.20	2925346.00	5.05
513120.80	2925425.00	5.76	513127.20	2925404.00	2.30	513142.34	2925346.00	5.05
513128.80	2925427.00	5.93	513134.20	2925401.00	2.32	513147.68	2925347.00	5.05
513134.60	2925429.00	6.05	513141.20	2925397.00	2.26	513153.54	2925348.00	5.04
513141.65	2925431.00	6.09	513149.90	2925401.00	2.50	513157.18	2925348.00	5.04
513151.68	2925433.00	6.14	513157.30	2925405.00	2.60	513161.30	2925349.00	5.04
513156.20	2925434.00	6.17	513162.96	2925407.00	2.08	513165.82	2925350.00	5.03
513163.69	2925436.00	6.13	513166.50	2925409.00	1.76	513170.16	2925350.00	5.03
513172.99	2925438.00	6.09	513175.00	2925406.00	1.62	513172.81	2925351.00	5.03
513178.00	2925439.00	6.07	513183.50	2925403.00	1.61	513176.10	2925351.00	5.02
513184.10	2925441.00	5.91	513189.90	2925403.00	1.54	513180.40	2925350.00	5.01
513190.63	2925441.00	5.82	513197.10	2925404.00	1.45	513184.37	2925349.00	4.99
513197.80	2925440.00	5.72	513205.70	2925404.00	1.38	513187.80	2925348.00	4.98
513211.50	2925439.00	5.81	513212.67	2925405.00	1.39	513194.90	2925347.00	4.96
513220.16	2925438.00	5.88	513217.40	2925406.00	1.40	513201.86	2925345.00	4.95
513228.30	2925438.00	5.93	513224.70	2925407.00	1.37	513208.06	2925344.00	4.94
513239.40	2925437.00	5.95	513230.90	2925408.00	1.34	513213.40	2925343.00	4.92
513245.97	2925437.00	5.93	513234.90	2925405.00	1.61	513217.79	2925342.00	4.91
513253.90	2925436.00	5.91	513241.20	2925400.00	1.65	513222.60	2925341.00	4.90
513258.57	2925434.00	5.93	513245.40	2925397.00	1.68	513226.34	2925340.00	4.90
513264.70	2925431.00	5.94	513250.84	2925396.00	1.56	513228.63	2925340.00	4.89

Authors' Contributions All authors contributed to the study's conception and design. Material preparation, data collection, and analysis were performed by Zohre Aghamolaei and Masoud-Reza Hesami Kermani. Zohre Aghamolaei: Writing - original draft. Masoud Reza Hesami Kermani: Writing - original draft, Project administration.

Funding No funding was received.

Availability of Data and Materials The codes are readily available from the authors on request.

Declarations

Competing Interests The authors declare that they have no known competing financial interests or personal relationships that could have appeared to influence the work reported in this paper.

References

- Afzali Ahmadabadi S, Jafari-Asl J, Banifakhr E, Houssein EH, Ben Seghier MEA (2023) Risk-Based Design Optimization of Contamination Detection Sensors in Water Distribution Systems: Application of an Improved Whale Optimization Algorithm. *Water* 15(12):2217
- Babaei M, Roozbahani A, Shahdany SMH (2018) Risk Assessment of Agricultural Water Conveyance and Delivery Systems by Fuzzy Fault Tree Analysis Method. *Water Resour Manag* 32(12):4079–4101
- Bailly du Bois P et al. (2012) In-Situ database toolbox for short-term dispersion model validation in macro-tidal seas, application for 2D-model. *Continental Shelf Research*, 36:63–82
- Ben Seghier MEA, Correia JA, Jafari-Asl J, Malekjafarian A, Plevris V, Trung NT (2021) On the modeling of the annual corrosion rate in main cables of suspension bridges using combined soft computing model and a novel nature-inspired algorithm. *Neural Comput Appl* 33(23):15969–15985
- Colbo K, Ross T, Brown C, Weber T (2014) A review of oceanographic applications of water column data from multibeam echosounders. *Estuar Coast Shelf Sci* 145:41–56
- Dey S, Saksena S, Merwade V (2019) Assessing the effect of different bathymetric models on hydraulic simulation of rivers in data sparse regions. *J Hydrol* 575:838–851
- Dikshit A, Pradhan B, Alamri AM (2020) Temporal Hydrological Drought Index Forecasting for New South Wales, Australia Using Machine Learning Approaches. *Atmosphere* 11(6):585
- Ebtehaj I, Bonakdari H, Safari MJS, Gharabaghi B, Zaji AH, Madavar HR et al (2020) Combination of sensitivity and uncertainty analyses for sediment transport modeling in sewer pipes. *Int J Sediment Res* 35(2):157–170
- Hardy RJ, Bates PD, Anderson MG (1999) The importance of spatial resolution in hydraulic models for floodplain environments. *J Hydrol* 216(1–2):124–136
- Intelmann SS (2006) Comments on hydrographic and topographic LIDAR acquisition and merging with multibeam sounding data acquired in the Olympic Coast National Marine Sanctuary
- Jafari-Asl J, Azizyan G, Monfared SAH, Rashki M, Andrade-Campos AG (2021) An enhanced binary dragonfly algorithm based on a V-shaped transfer function for optimization of pump scheduling program in water supply systems (case study of Iran). *Eng Fail Anal* 123:105323
- Jafari-Asl J, Seghier MEAB, Ohadi S, van Gelder P (2021) Efficient method using Whale Optimization Algorithm for reliability-based design optimization of labyrinth spillway. *Applied Soft Computing* 101:107036
- Lai R, Wang M, Yang M, Zhang C (2018) Method based on the Laplace equations to reconstruct the river terrain for two-dimensional hydrodynamic numerical modeling. *Comput Geosci* 111:26–38
- Langridge M, Gharabaghi B, McBean E, Bonakdari H, Walton R (2020) Understanding the dynamic nature of time-to-peak in UK Streams. *J Hydrol* 583:124630
- Larson M (2005) Numerical Modeling. In: Schwartz, M.L. (eds) Encyclopedia of Coastal Science. Encyclopedia of Earth Science Series. Springer, Dordrecht. https://doi.org/10.1007/1-4020-3880-1_232
- Li J, Heap AD (2011) A review of comparative studies of spatial interpolation methods in environmental sciences: Performance and impact factors. *Ecol Inform* 6(3–4):228–241
- Liu et al. (2018) Reduced resilience as a potential early warning signal of forest mortality ecological society of America annual meeting 5(10)

- Mai SH, Ben Seghier ME, Nguyen PL, Jafari-Asl J, Thai DK (2020) A hybrid model for predicting the axial compression capacity of square concrete-filled steel tubular columns. *Eng Comp* 1–18
- Merwade VM, Maidment DR, Hodges BR (2005) Geospatial representation of river channels. *J Hydrol Eng* 10(3):243–251
- Modaresi et al. (2018) An approach for improving the accuracy of monthly streamflow forecasting. *J Hydroinformatics* 20(4):917–933
- Nittrouer JA, Allison MA, Campanella R (2008) Evaluation of bedload transport in the lower Mississippi River: implications for sand transport to the Gulf of Mexico. *J Geophys Res Earth Surf* 113:F03004
- Noori N, Kalin L (2016) Coupling SWAT and ANN models for enhanced daily streamflow prediction. *J Hydrol Eng* 533:141–151
- Ohadi S, Jafari-Asl J (2021) Multi-objective reliability-based optimization for design of trapezoidal labyrinth weirs. *Flow Meas Instrum* 77:101787
- Podhorányi M, Unucka J, Bobál' P, Říhová V (2013) Effects of LiDAR DEM resolution in hydrodynamic modelling: model sensitivity for cross-sections. *Int J Digit Earth* 6(1):3–27
- Quarteroni A, Quarteroni S (2009) Numerical models for differential problems, vol 2. Springer, Milan
- Rahmanshahi M, Jafari-Asl J, Shafai Bejestan M, Mirjalili S (2023) A Hybrid Model for Predicting the Energy Dissipation on the Block Ramp Hydraulic Structures. *Water Resources Management* 37(8):3187–3209
- Raber GT, Jensen JR, Hodgson ME, Tullis JA, Davis BA, Berglund J (2007) Impact of LiDAR nominal post-spacing on DEM accuracy and flood zone delineation. *Photogramm Eng Remote Sensing* 73(7):793–804
- Rad et al. (2022) A Radial Basis Function Neural Network Approach to Predict Preschool Teachers' Technology, Acceptance Behavior, *Frontiers in Psychology* 13:880753
- Riahi-Madvar H, Dehghani M, Memarzadeh R, Gharabaghi B (2021) Short to long-term forecasting of river flows by heuristic optimization algorithms hybridized with ANFIS. *Water Resour Manag* 35(4):1149–1166
- Seo Y, Kim S, Kisi O, Singh VP (2015) Daily water level forecasting using wavelet decomposition and artificial intelligence techniques. *J Hydrol* 520:224–243
- Sharifi H, Roozbahani A, Hashemy Shahdany SM (2021) Evaluating the performance of agricultural water distribution systems using FIS, ANN and ANFIS intelligent models. *Water Resour Manag* 35(6):1797–1816
- Vogel, Marker (2010) Revised Modelling of the Post-Ad 79 Volcanic Deposits of Somma-Vesuvius to Reconstruct the Pre-Ad 79 Topography of the Sarno River Plain 5–16
- Walton R, Binns A, Bonakdari H, Ebtehaj I, Gharabaghi B (2019) Estimating 2-year flood flows using the generalized structure of the group method of data handling. *J Hydrol* 575:671–689
- Yongfei Fu, Liu Yuyu, Shigu Xu, Zhenghe Xu (2022) Assessment of a Multifunctional River Using Fuzzy Comprehensive Evaluation Model in Xiaoqing River, Eastern China. *Int J Environ Res Public Health* 19:12264

Publisher's Note Springer Nature remains neutral with regard to jurisdictional claims in published maps and institutional affiliations.

Springer Nature or its licensor (e.g. a society or other partner) holds exclusive rights to this article under a publishing agreement with the author(s) or other rightsholder(s); author self-archiving of the accepted manuscript version of this article is solely governed by the terms of such publishing agreement and applicable law.